

Decay spectroscopy of  $^{160}\text{Sm}$ : The lightest four-quasiparticle  $K$  isomer

Z. Patel<sup>a,b,\*</sup>, Zs. Podolyák<sup>a</sup>, P.M. Walker<sup>a</sup>, P.H. Regan<sup>a,c</sup>, P.-A. Söderström<sup>b</sup>,  
 H. Watanabe<sup>b,d,e</sup>, E. Ideguchi<sup>f,g</sup>, G.S. Simpson<sup>h</sup>, S. Nishimura<sup>b</sup>, F. Browne<sup>b,j</sup>,  
 P. Doornenbal<sup>b</sup>, G. Lorusso<sup>b,c</sup>, S. Rice<sup>a,b</sup>, L. Sinclair<sup>b,k</sup>, T. Sumikama<sup>l</sup>, J. Wu<sup>b,i</sup>, Z.Y. Xu<sup>m</sup>,  
 N. Aoi<sup>f,g</sup>, H. Baba<sup>b</sup>, F.L. Bello Garrote<sup>n</sup>, G. Benzoni<sup>o</sup>, R. Daido<sup>g</sup>, Zs. Dombrádi<sup>v</sup>, Y. Fang<sup>g</sup>,  
 N. Fukuda<sup>b</sup>, G. Gey<sup>h</sup>, S. Go<sup>p</sup>, A. Gottardo<sup>q</sup>, N. Inabe<sup>b</sup>, T. Isobe<sup>b</sup>, D. Kameda<sup>b</sup>,  
 K. Kobayashi<sup>r</sup>, M. Kobayashi<sup>p</sup>, T. Komatsubara<sup>s,t</sup>, I. Kojouharov<sup>u</sup>, T. Kubo<sup>b</sup>, N. Kurz<sup>u</sup>,  
 I. Kuti<sup>v</sup>, Z. Li<sup>w</sup>, H.L. Liu<sup>x</sup>, M. Matsushita<sup>p</sup>, S. Michimasa<sup>p</sup>, C.-B. Moon<sup>y</sup>, H. Nishibata<sup>g</sup>,  
 I. Nishizuka<sup>l</sup>, A. Odahara<sup>g</sup>, E. Şahin<sup>n</sup>, H. Sakurai<sup>b,m</sup>, H. Schaffner<sup>u</sup>, H. Suzuki<sup>b</sup>,  
 H. Takeda<sup>b</sup>, M. Tanaka<sup>g</sup>, J. Taprogge<sup>z,aa</sup>, Zs. Vajta<sup>v</sup>, F.R. Xu<sup>i</sup>, A. Yagi<sup>g</sup>, R. Yokoyama<sup>p</sup>

<sup>a</sup> Department of Physics, University of Surrey, Guildford, GU2 7XH, United Kingdom

<sup>b</sup> RIKEN Nishina Center, 2-1 Hirosawa, Wako-shi, Saitama 351-0198, Japan

<sup>c</sup> National Physical Laboratory, Teddington, Middlesex, TW11 0LW, United Kingdom

<sup>d</sup> International Research Center for Nuclei and Particles in the Cosmos, Beihang University, Beijing 100191, China

<sup>e</sup> School of Physics and Nuclear Energy Engineering, Beihang University, Beijing 100191, China

<sup>f</sup> Research Center for Nuclear Physics (RCNP), Osaka University, Ibaraki, Osaka 567-0047, Japan

<sup>g</sup> Department of Physics, Osaka University, Machikaneyama-machi 1-1, Osaka 560-0043 Toyonaka, Japan

<sup>h</sup> LPSC, Université Joseph Fourier Grenoble 1, CNRS/IN2P3, Institut National Polytechnique de Grenoble, F-38026 Grenoble Cedex, France

<sup>i</sup> School of Physics and State Key Laboratory of Nuclear Physics and Technology, Peking University, Beijing 100871, China

<sup>j</sup> School of Computing, Engineering and Mathematics, University of Brighton, Brighton, BN2 4JG, United Kingdom

<sup>k</sup> Department of Physics, University of York, Heslington, York, YO10 5DD, United Kingdom

<sup>l</sup> Department of Physics, Tohoku University, Aoba, Sendai, Miyagi 980-8578, Japan

<sup>m</sup> Department of Physics, University of Tokyo, Hongo, Bunkyo-ku, Tokyo 113-0033, Japan

<sup>n</sup> Department of Physics, University of Oslo, Oslo, Norway

<sup>o</sup> INFN Sezione di Milano, I-20133 Milano, Italy

<sup>p</sup> Center for Nuclear Study (CNS), University of Tokyo, Wako, Saitama 351-0198, Japan

<sup>q</sup> Istituto Nazionale di Fisica Nucleare, Laboratori Nazionali di Legnaro, I-35020 Legnaro, Italy

<sup>r</sup> Department of Physics, Rikkyo University, 3-34-1 Nishi-Ikebukuro, Toshima-ku, Tokyo 171-8501, Japan

<sup>s</sup> Research Facility Center for Pure and Applied Science, University of Tsukuba, Ibaraki 305-8577, Japan

<sup>t</sup> Rare Isotope Science Project, Institute for Basic Science, Daejeon 305-811, Republic of Korea

<sup>u</sup> GSI Helmholtzzentrum für Schwerionenforschung GmbH, 64291 Darmstadt, Germany

<sup>v</sup> Institute for Nuclear Research, Hungarian Academy of Sciences, P.O. Box 51, Debrecen, H-4001, Hungary

<sup>w</sup> School of Physics, Peking University, Beijing 100871, China

<sup>x</sup> Department of Applied Physics, School of Science, Xi'an Jiaotong University, Xi'an 710049, China

<sup>y</sup> Hoseo University, Asan, Chungnam 336-795, Republic of Korea

<sup>z</sup> Instituto de Estructura de la Materia, CSIC, E-28006 Madrid, Spain

<sup>aa</sup> Departamento de Física Teórica, Universidad Autónoma de Madrid, E-28049 Madrid, Spain

## ARTICLE INFO

## Article history:

Received 30 June 2015

Received in revised form 14 October 2015

Accepted 8 December 2015

Available online 11 December 2015

Editor: D.F. Geesaman

## ABSTRACT

The decay of a new four-quasiparticle isomeric state in  $^{160}\text{Sm}$  has been observed using  $\gamma$ -ray spectroscopy at the RIBF, RIKEN. The four-quasiparticle state is assigned a  $2\pi \otimes 2\nu \pi \frac{5}{2}^- [532]$ ,  $\pi \frac{5}{2}^+ [413]$ ,  $\nu \frac{5}{2}^- [523]$ ,  $\nu \frac{7}{2}^+ [633]$  configuration. The half-life of this  $(11^+)$  state is measured to be  $1.8(4) \mu\text{s}$ . The  $(11^+)$  isomer decays into a rotational band structure, based on a  $(6^-)$   $\nu \frac{5}{2}^- [523] \otimes \nu \frac{7}{2}^+ [633]$  bandhead, consistent with the  $g_K - g_R$  values. This decays to a  $(5^-)$  two-proton quasiparticle state, which in turn decays to the ground state band. Potential energy surface and blocked-BCS calculations were performed in the deformed midshell region around  $^{160}\text{Sm}$ . They reveal a significant influence from  $\beta_6$  deformation

\* Corresponding author at: Department of Physics, University of Surrey, Guildford, GU2 7XH, United Kingdom.

E-mail address: z.patel@surrey.ac.uk (Z. Patel).

and that  $^{160}\text{Sm}$  is the best candidate for the lightest four-quasiparticle  $K$  isomer to exist in this region. The relationship between reduced hindrance and isomer excitation energy for E1 transitions from multi-quasiparticle states is considered with the new data from  $^{160}\text{Sm}$ . The E1 data are found to agree with the existing relationship for E2 transitions.

© 2015 Published by Elsevier B.V. This is an open access article under the CC BY license (<http://creativecommons.org/licenses/by/4.0/>). Funded by SCOAP<sup>3</sup>.

The existence of nuclear metastable, or isomeric, states with half-lives of nanoseconds or longer provides a useful tool, enabling spectroscopic investigation of intrinsic and collective states within a nucleus that might otherwise be difficult to observe. In combination with projectile fragmentation and fission reactions, isomers can give unique access to the high-spin excited-state structure of neutron-rich nuclei, but only if suitable high-spin isomers exist. Therefore, understanding the formation and stability of multi-quasiparticle isomers is a key part of fully exploiting the new generation of radioactive-beam facilities.

The projection of the angular momentum of a nucleus on its symmetry axis is known as the  $K$  quantum number.  $K$  isomerism arises from axially symmetric deformation in the nucleus, enabling the nucleus to be ‘trapped’ in an aligned spin orientation relative to its symmetry axis [1].  $K$ -isomeric states appear systematically in neutron-rich nuclei with  $A \geq 150$  which typically have deformed prolate shapes. The nucleus is isomeric when the transition to a lower energy state with a different  $K$  value is inhibited by the  $\Delta K \leq \lambda$  selection rule, where  $\lambda$  is the multipole order of the transition. These transitions are able to proceed through symmetry-breaking processes, where the hindrance factor is strongly correlated with the degree of forbiddenness,  $\nu = \Delta K - \lambda$ . The partial half-life of the isomeric state relative to the single-particle Weisskopf estimate is known as the reduced hindrance of a transition, expressed as  $f_\nu = (T_{1/2}^Y/T_{1/2}^W)^{1/\nu}$  [1].

$K$  isomers may arise from the breaking of one or more coupled nucleon pairs to form multi-quasiparticle (multi-qp) states. The excitation energy and other properties of these states depend strongly on the number of proton and neutron states involved [2]. Prior to this work,  $^{164}\text{Er}$  ( $Z = 68$ ,  $N = 96$ ) was the lightest nucleus with a known four-qp  $K$  isomeric state [3]. Many two-qp isomeric states have been discovered in nuclei lighter than  $^{164}\text{Er}$ , for example, in  $^{156,158,160,164}\text{Sm}$  ( $Z = 62$ ) [4–7],  $^{152,154,156}\text{Nd}$  ( $Z = 60$ ) [6,8–11], and  $^{166}\text{Gd}$  ( $Z = 64$ ) [7], but none  $\geq$  four-qp. Increasingly more neutron-rich isotopes must be populated to further probe this region. The radioactive isotope beam factory, RIBF, at RIKEN has more recently enabled population of these nuclei using high uranium beam intensities.

Nuclei around  $^{160}\text{Sm}$  were populated by in-flight fission of a  $345 \text{ A} \cdot \text{MeV}$   $^{238}\text{U}$  beam incident on a 4 mm thick  $^9\text{Be}$  target at the RIBF. The beam intensity at the target was 10 particle-nA on average. The secondary radioactive isotope beam containing the nuclei of interest was passed through the BigRIPS and ZeroDegree spectrometers: a two-stage achromatic separation system that separates and identifies the beam species on an ion by ion basis, using time-of-flight, magnetic rigidity and energy loss (TOF-B $\rho$ - $\Delta E$ ) [12,13].

Delayed  $\gamma$  rays were detected from the isomeric decay of the tagged ions using EURICA (Euroball-RIKEN Cluster Array) [14–16]: 84 HPGe crystals arranged in a  $4\pi$  configuration around a copper passive stopper. The absolute efficiency of the array was 16.6% at 100 keV and 7.6% at 1 MeV. A 100  $\mu\text{s}$  time coincidence window was used to correlate ion implantation to  $\gamma$ -ray detection.

Delayed  $\gamma$  rays from the isomeric decay of  $^{160}\text{Sm}$  are shown in Fig. 1. All labelled peaks have been identified and placed in the level scheme. A previous experiment by Simpson et al. [6] had

identified a ( $5^-$ ) two-qp isomer that decays via 878 and 1128 keV transitions to the  $6^+$  and  $4^+$  states in the ground state band respectively. In addition to these transitions,  $\gamma$  rays from the decay of a four-qp isomer are now observed in the current work. In particular a strongly-coupled rotational band structure is newly identified. These new  $\gamma$  rays have been added to the  $^{160}\text{Sm}$  level scheme, presented in Fig. 2.

The level scheme was deduced from  $\gamma$ - $\gamma$  coincidence analysis. The new  $\gamma$  rays with the highest energy (432 and 641 keV) were determined to depopulate the isomeric state directly. The  $2^+ \rightarrow 0^+$  71 keV  $\gamma$  ray cannot be observed in Fig. 1 due to a strongly competing electron conversion process, but has been observed in coincident spectra. In addition to the  $\gamma$  rays placed in the  $^{160}\text{Sm}$  level scheme, weak  $\gamma$  rays at 123, 149, and 316 keV are also observed in Fig. 1, but were unable to be placed due to low statistics in the coincident spectra.

The spin and parity assignments in Fig. 2 are determined from the transition multiplicities, which have been obtained from the intensity balances through the levels and the decay patterns. The intensities can be seen in Table 1. The intensity is not required to balance when transitioning through the ( $5^-$ ) isomeric state. The spin and parity assignments are tentative in the absence of directly measured electron conversion coefficients and  $\gamma$ -ray angular correlations.

The half-life of the four-qp isomeric state was measured to be  $1.8(4) \mu\text{s}$ , from the weighted average of the 432 and 641 keV  $\gamma$ -ray half-lives. The half-lives were measured from the exponential decay curves derived from the time between ion implantation and  $\gamma$ -ray detection (see inset in Fig. 1). The half-life of the ( $5^-$ ) two-qp state was previously measured at 120(46) ns [6]. The half-life of this isomeric state was not measured in this work as the statistics were not sufficient to resolve the two different half-lives.

Two  $\gamma$  rays of 432 and 641 keV depopulate the four-qp isomer into a band structure built on a two-qp bandhead. A spin of at least  $11\hbar$  for the four-qp state is required by the absence of a transition from the isomeric state to the ( $9^-$ ) state. Spin-parities of  $11^+$  and  $12^-$  are permitted by the experimental data. Our calculations presented below suggest a  $K^\pi = 11^+$  assignment for the four-qp state.

To further understand the level scheme blocked-BCS calculations [17] were performed. BCS theory treats the nucleus as a superfluid, where the presence of unpaired particles affects the superfluidity through a ‘‘blocking effect’’. In this work the pairing strengths were fixed as  $G_\pi = 21.00 \text{ A} \cdot \text{MeV}$  and  $G_\nu = 20.00 \text{ A} \cdot \text{MeV}$ , in accordance with Jain et al. [17]. The Nilsson energies were then calculated for a set of deformation parameters;  $\epsilon_2 = 0.267$  and  $\epsilon_4 = -0.027$ , taken from Möller et al. [18]. The results can be seen in Table 2.

These calculations show that a  $6^-$  neutron state with a  $\nu \frac{5}{2}^- [523] \otimes \nu \frac{7}{2}^+ [633]$  configuration and a  $5^-$  proton state with a  $\pi \frac{5}{2}^- [532] \otimes \pi \frac{5}{2}^+ [413]$  configuration are the lowest energy two-qp states. The combination of these states forms an  $11^+$  four-qp state. The two-qp state depopulated by the 878 and 1128 keV transitions was previously suggested to be a ( $5^-$ ) state arising from a two-neutron  $\nu \frac{5}{2}^+ [642] \otimes \nu \frac{5}{2}^- [523]$  configuration [6]. However, our

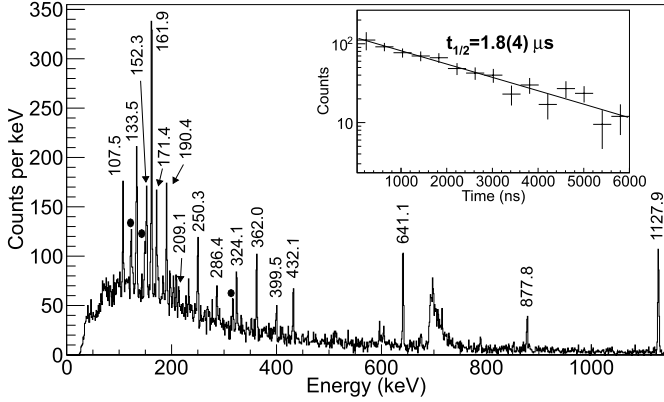


**Fig. 1.** Energy spectrum of delayed  $\gamma$  rays from  $^{160}\text{Sm}$  observed 0.5 to 2.5  $\mu\text{s}$  following implantation. All labelled  $\gamma$  rays have been placed in the level scheme. Those marked with filled circles are the 123, 149, and 316 keV  $\gamma$  rays that were unable to be placed in the level scheme. Inset: The exponential decay curve from the four-quasiparticle isomeric decay of  $^{160}\text{Sm}$ , obtained from the 432 and 641 keV  $\gamma$  rays.

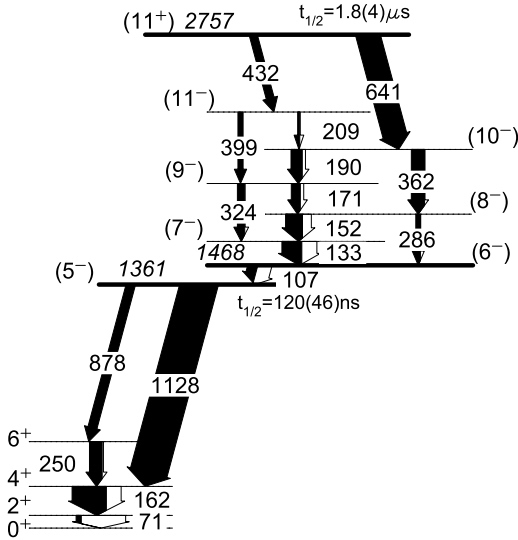


**Fig. 2.** Level scheme of  $^{160}\text{Sm}$ . All  $\gamma$  rays above the  $(5^-)$  two-qp state are new. The half-life of the  $(5^-)$  state is from Ref. [6].

blocked-BCS calculations show that a  $5^-$  two-proton configuration is preferred.

The branching ratios in a band can be used to infer the band-head configuration. The difference between the expected and experimental intrinsic  $g$  factor ( $g_K$ ) can indicate whether a band structure is built on a proton or a neutron bandhead.

The expected intrinsic  $g$  factor is calculated from  $Kg_K = \Sigma(g_\Lambda \Lambda + g_\Sigma \Sigma)$ , where  $\Lambda$  and  $\Sigma$  are the projections of the orbital angular momentum and intrinsic spin on the symmetry axis respectively, and  $g_\Lambda$  and  $g_\Sigma$  are the corresponding  $g$  factors.  $g_\Lambda$  is 0 for neutrons and 1 for protons, and  $g_\Sigma$  is 4.99 for protons and  $-3.23$  for neutrons; attenuated from their free values by a factor of 0.6 [19]. Our BCS calculations have revealed a  $6^-$  two-qp state is lowest in energy for neutrons and a  $5^-$  two-qp state is lowest in energy for protons. The expected  $g_K$  for these configurations is 0 and 1 respectively. The experimental values for  $g_K$  are found using the following:

$$\frac{|g_K - g_R|}{Q_0} = 0.933 \frac{E_1}{\delta \sqrt{I^2 - 1}}$$

where  $g_R$  is the rotational  $g$  factor, taken as 0.3 [19],  $Q_0$  is the intrinsic quadrupole moment, taken to be  $7.0 e \cdot b$  from Sm sys-

**Table 1**

Initial level energy,  $E_i$ , spin-parity,  $J_i^\pi$ , and branching ratio,  $B_{\text{tot}}$  (corrected for electron conversion) of the levels obtained for  $^{160}\text{Sm}$  in this work. For each  $\gamma$  ray the energy,  $E_\gamma$ ,  $\gamma$ -ray intensity,  $I_\gamma$  relative to the 1128 keV  $\gamma$ -ray intensity, and final level spin,  $J_f^\pi$ , are listed.

$E_i$ (keV)	$J_i^\pi$	$E_\gamma$ (keV)	$I_\gamma$ (rel.)	$B_{\text{tot}}$ (rel.)	$J_f^\pi$
71	$2^+$	71(1) <sup>a</sup>		100	$0^+$
232.9	$4^+$	161.9(3)	91(11)	100	$2^+$
483.2	$6^+$	250.3(4)	34(6)	100	$4^+$
1361.0	$(5^-)$	877.8(4)	24(5)	20(5)	$6^+$
		1127.9(4)	100	80(19)	$4^+$
1468.5	$(6^-)$	107.5(3)	26(5)	100	$(5^-)$
1602.0	$(7^-)$	133.5(3)	53(8)	100	$(6^-)$
1754.3	$(8^-)$	152.3(4)	45(9)	84(25)	$(7^-)$
		286.4(4)	12(3)	16(5)	$(6^-)$
1925.7	$(9^-)$	171.4(4)	24(5)	62(17)	$(8^-)$
		324.1(4)	20(5)	38(11)	$(7^-)$
2116.1	$(10^-)$	190.4(4)	30(6)	51(12)	$(9^-)$
		362.0(3)	35(6)	49(11)	$(8^-)$
2325.2	$(11^-)$	209.1(5)	6(4)	33(25)	$(10^-)$
		399.5(5)	13(4)	67(52)	$(9^-)$
2757.3	$(11^+)$	432.1(4)	21(5)	25(6)	$(10^-)$
		641.1(3)	64(9)	75(18)	$(11^-)$

<sup>a</sup> The 71 keV  $\gamma$  ray is only observed in coincident spectra.

**Table 2**

Low-lying quasiparticle states in  $^{160}\text{Sm}$  predicted by blocked-BCS calculations (marked with a B) and potential energy surface calculations (marked with a P). The potential energy surface calculations have only been performed for the lowest energy states.

$K^\pi$	Configuration	$E_x^{\text{B}}(E_x^{\text{P}})$ (MeV)	$E_x^{\text{EXP}}$ (MeV)
$\nu$ two-qp			
$6^-$	$\nu \frac{5}{2}^- [523] \otimes \nu \frac{7}{2}^+ [633]$	1.401 (1.727 <sup>a</sup> )	1.468
$3^+$	$\nu \frac{5}{2}^- [523] \otimes \nu \frac{1}{2}^- [521]$	1.674 <sup>b</sup>	
$5^+$	$\nu \frac{5}{2}^- [523] \otimes \nu \frac{5}{2}^- [512]$	1.953	
$3^-$	$\nu \frac{1}{2}^- [521] \otimes \nu \frac{5}{2}^+ [642]$	2.115	
$\pi$ two-qp			
$5^-$	$\pi \frac{5}{2}^- [532] \otimes \pi \frac{5}{2}^+ [413]$	1.032 (1.457 <sup>a</sup> )	1.361
$4^-$	$\pi \frac{5}{2}^- [532] \otimes \pi \frac{3}{2}^- [411]$	1.569 <sup>b</sup>	
$4^+$	$\pi \frac{5}{2}^+ [413] \otimes \pi \frac{3}{2}^- [411]$	1.631	
$4^-$	$\pi \frac{5}{2}^+ [413] \otimes \pi \frac{3}{2}^- [541]$	2.107	
four-qp			
$11^+$	$\nu \frac{5}{2}^- [523] \otimes \nu \frac{7}{2}^+ [633],$ $\pi \frac{5}{2}^- [532] \otimes \pi \frac{5}{2}^+ [413]$	2.433 (3.214 <sup>a</sup> )	2.757
$8^-$	$\nu \frac{5}{2}^- [523] \otimes \nu \frac{1}{2}^- [521],$ $\pi \frac{5}{2}^- [532] \otimes \pi \frac{5}{2}^+ [413]$	2.706 <sup>b</sup>	
$10^+$	$\nu \frac{5}{2}^- [523] \otimes \nu \frac{7}{2}^+ [633],$ $\pi \frac{5}{2}^- [532] \otimes \pi \frac{3}{2}^- [411]$	2.970 <sup>b</sup>	

<sup>a</sup>  $(\beta_2, \beta_4, \beta_6) = (0.294, 0.052, -0.017), (0.287, 0.046, -0.011),$  and  $(0.290, 0.048, -0.013)$  for  $K^\pi = 6^-, 5^-,$  and  $11^+$  states respectively.

<sup>b</sup> 200 keV has been added to these states as they have energetically unfavoured configurations according to the residual spin-spin coupling rule.

tematics, and  $E_1$  is the energy of the  $M1/E2$  mixed transition in MeV from an initial state with spin  $I$ . The quadrupole/dipole mixing ratio,  $\delta$ , is calculated using the formula:

$$q = \frac{\delta^2}{1 + \delta^2} = \frac{2K^2(2I - 1)}{(I - K - 1)(I + K - 1)(I + 1)} \frac{E_1^5}{E_2^2} \lambda_b$$

where  $\lambda_b$  is the  $\gamma$ -ray branching ratio and  $E_2$  is the energy of the  $E2$  transition from the initial state. The results can be seen in Table 3. Two values of  $g_K$  are given due to the rearrangement of the modulus,  $|g_K - g_R|$  in the above equation. These values show that the bandhead regardless of  $K^\pi$  must be comprised of a two-

**Table 3**

Experimental  $g_K$  values for various transitions in  $^{160}\text{Sm}$ , considering  $K = 5$  and  $K = 6$  bandheads. Two values exist due to the modulus  $|g_K - g_R|$ . Theoretical values are  $g_K = 0$  for neutrons and  $g_K = 1$  for protons.

$K^\pi$	$J_i^\pi$	$E_1$ and $E_2$ (keV)	$g_K^{exp}$
$5^-$	$11^-$	209 and 399	-0.11(27), 0.71(26)
$5^-$	$10^-$	190 and 362	-0.12(14), 0.72(14)
$5^-$	$9^-$	171 and 324	-0.10(16), 0.70(16)
$5^-$	$8^-$	152 and 286	-0.24(23), 0.84(23)
$5^-$	weighted average		-0.13(16), 0.73(16)
$6^-$	$11^-$	209 and 399	0.00(20), 0.60(20)
$6^-$	$10^-$	190 and 362	0.00(10), 0.61(10)
$6^-$	$9^-$	171 and 324	0.03(11), 0.57(11)
$6^-$	$8^-$	152 and 286	-0.13(37), 0.73(37)
$6^-$	weighted average		-0.01(16), 0.61(16)

neutron state, as they are consistent with the theoretical value of  $g_K = 0$ , but not with  $g_K = 1$ .

The assignment of a ( $6^-$ ) neutron bandhead for the main band structure, rather than a ( $5^-$ ) neutron bandhead is made on the basis of a lack of observation of a transition from the  $7^-$  state to the  $5^-$ , which would have an energy of 240 keV. The expected  $\gamma$ -ray intensity of this transition was calculated using the g-factor formula, rearranged for  $I_\gamma$  and found to be 570(70) counts (assuming  $E2$  multipolarity). This transition, if present, would be easily observable in the  $\gamma$ -ray energy spectrum, with  $I_\gamma(\text{rel.}) = 12(2)$ , comparable to the 286 keV peak. As we do not observe this peak, we assign the bandhead to the ( $6^-$ ) state rather than the ( $5^-$ ) state.

It has been noted in this mass region that  $\beta_6$  deformation can be significant [18] and can have a measurable effect on the structure of the nucleus [7]. In order to quantify this effect potential energy surface calculations were performed on  $^{160}\text{Sm}$  and its neighbouring nuclei. The total energy of the configurations was minimised in  $(\beta_2, \beta_4)$  deformation space and  $(\beta_2, \beta_4, \beta_6)$  deformation space. For more details see Refs. [20,21]. The inclusion of  $\beta_6$  in the calculations has the greatest effect on the  $6^-$  2-neutron state in  $^{160}\text{Sm}$ , where the energy is reduced by 100 keV. Conversely, the energy of the  $5^-$  2-proton state increases by 50 keV with the inclusion of  $\beta_6$ , enabling the  $6^-$  state to compete. Consequently,  $\beta_6$  plays a role in moving the calculated  $6^-$  and  $5^-$  bandheads closer together in energy. The energies of the assigned bandheads calculated using  $(\beta_2, \beta_4, \beta_6)$  deformation space are shown in Table 2.

The reduced hindrance of a transition removes the dependence of the half-life on energy and the multipole order,  $\lambda$ , of the transition. Therefore we would expect similar reduced hindrance values for isomers around  $^{160}\text{Sm}$ . However, a systematic study of  $E1$  transitions reveals an  $f_\nu$  dependence on  $E - E_R$ , similar to that known for  $E2$  transitions [29], where  $E$  is the energy of the isomeric state and  $E_R$  is the rigid rotor energy for the same angular momentum.

**Table 4**

Data summary of four-qp and higher-order-qp isomers with  $E1$  transitions used in Fig. 3. Those marked with \* have 0.9 MeV added to account for pairing energy.

Nucleus	$K^\pi$	$t_{1/2}$	$E_\gamma$ (keV)	$E$ (MeV)	$E - E_R$ (MeV)	$\nu$	$f_\nu$
$^{160}\text{Sm}$	( $11^+$ )	1.8(4) $\mu\text{s}$	641	2.78	1.83	4	22
$^{160}\text{Sm}$	( $11^+$ )	1.8(4) $\mu\text{s}$	432	2.78	1.83	4	21
$^{164}\text{Er}$ [24]	$12^+$	68(2) ns	555	3.38	2.33	4	9.4
$^{173}\text{Tm}$ [27]	$35/2^-$	121(28) ns	655	4.05	2.95*	6	8.3
$^{174}\text{Yb}$ [25,26]	$14^+$	55(4) ns	786	3.70	2.42	6	9.9
$^{174}\text{Hf}$ [23]	$14^+$	3.7 $\mu\text{s}$	379	3.31	2.03	5	15
$^{174}\text{Hf}$ [23]	$14^+$	3.7 $\mu\text{s}$	155	3.31	2.03	7	8.9
$^{175}\text{Hf}$ [23]	$45/2^+$	2 $\mu\text{s}$	291	4.64	2.34*	4	19
$^{182}\text{Hf}$ [22]	( $13^+$ )	40(10) $\mu\text{s}$	264	2.57	1.54	4	24
$^{179}\text{W}$ [19]	$35/2^-$	750(80) ns	625	3.35	2.36*	12	4.1
$^{183}\text{Os}$ [28]	$43/2^-$	27(3) ns	351	5.07	3.25*	4	4.9

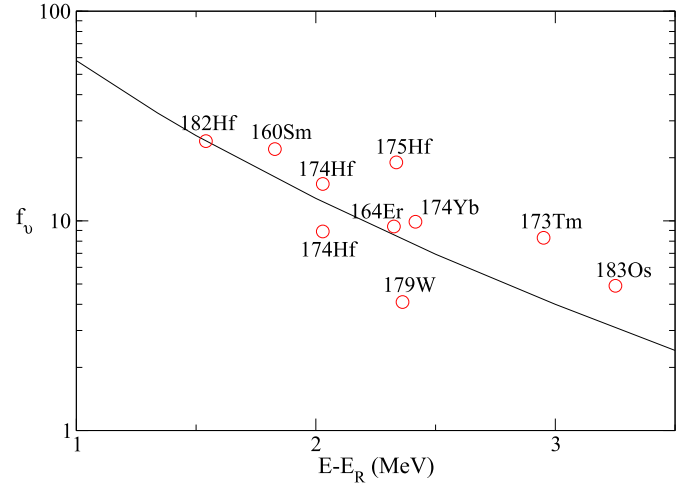


**Fig. 3.** Reduced hindrance,  $f_\nu$ , of  $E1$  transitions versus the difference between excitation energy of the isomeric state and the rigid rotor energy. Data points taken from Refs. [19,22–28] and the current work. A pairing energy of 0.9 MeV has been added to odd- $A$  nuclei.

The rigid rotor energy of  $^{160}\text{Sm}$  was calculated to be 927 keV, using a moment of inertia of  $71\hbar^2 \text{ MeV}^{-1}$ , found by scaling with  $A^{5/3}$  using  $85\hbar^2 \text{ MeV}^{-1}$  for  $^{178}\text{Hf}$ . For the ( $11^+$ ) isomer this gives  $E - E_R = 1.83 \text{ MeV}$ .

The reduced hindrances of the 432 and 641 keV transitions, and the 878 and 1128 keV transitions were calculated. All four  $E1$  transitions have very similar reduced hindrance values of 21(1), 22(1), 21(2) and 18(2) for 432, 641, 878, and 1128 keV respectively. Following common practice [22–24,27],  $F_W$  has been divided by  $10^4$  in an attempt to allow for the hindered nature of  $K$ -allowed  $E1$  transitions.

A plot of  $f_\nu$  versus  $E - E_R$  can be seen in Fig. 3 for  $E1$  transitions with  $\nu \geq 4$ . Isomers with  $\nu < 4$  are less forbidden and therefore excluded. The data are summarised in Table 4. The solid line in the plot is taken from statistical calculations for  $E2$  transitions [29]. The data from  $E1$  transitions, including the new data point from the four-qp isomer in  $^{160}\text{Sm}$  agree well with this trend. This relationship is evidence that reduced hindrance is sensitive to the excitation energy of the four-qp isomeric state. This could be due to greater  $K$  mixing at higher excitation energies: the density of states increases with excitation energy which statistically leads to more states with the same spin and parity to mix with [29]. To further test this relationship, data on lighter deformed isomers with four-qp states are required.

To date,  $^{160}\text{Sm}$  is the lightest four-qp  $K$  isomer observed. Blocked-BCS calculations were performed on lighter nuclei in this region to test the limits of existence of four-qp isomers. The next best candidate is predicted to be a four-qp isomer in  $^{158}\text{Sm}$ , with

$K^\pi = 10^+$  and  $E = 2.424$  MeV. However, to date only a two-qp isomeric state has been observed in this nucleus [3]. Due to the lower spin, the predicted four-qp isomer in  $^{158}\text{Sm}$  would likely have a shorter half-life than that of  $^{160}\text{Sm}$ . Overall, the calculations show that  $^{160}\text{Sm}$  is the strongest candidate for the lightest four-qp isomer to exist in this region, consistent with our new observations.

In summary, a new four-qp isomer has been observed in  $^{160}\text{Sm}$  with a half-life of  $1.8(4)$   $\mu\text{s}$ . The level scheme has been extended using the present spectroscopic data. This is the lightest four-qp  $K$  isomer observed to date. The new data from  $^{160}\text{Sm}$  agree well with the inverse correlation between reduced hindrance and excitation energy for  $E1$  and  $E2$  transitions, shown here for the first time for  $E1$  transitions. Blocked-BCS calculations reveal  $^{160}\text{Sm}$  and  $^{158}\text{Sm}$  are the best candidates for deformed four-qp isomers. However, further experiments are needed to ascertain the  $Z$  and  $N$  limits for their existence.

### Acknowledgements

This work was carried out at the RIBF operated by RIKEN Nishina Center, RIKEN and CNS, University of Tokyo. All UK authors are supported by STFC. P.H.R. and G.L. are partially supported by the UK National Measurement Office (NMO). P.-A.S. was financed by JSPS Grant Number 23.01752 and the RIKEN Foreign Postdoctoral Researcher Program. J.T. was financed by Spanish Ministerio de Ciencia e Innovación under Contracts No. FPA2009-13377-C02 and No. FPA2011-29854-C04. Zs.D., I.K., and Zs.V. were supported by OTKA contract number K100835. We acknowledge the EUROBALL Owners Committee for the loan of germanium detectors and the PreSpec Collaboration for the readout electronics of the

cluster detectors. This work was supported by JSPS KAKENHI Grant No. 25247045.

### References

- [1] P. Walker, G. Dracoulis, *Nature* 399 (1999) 35.
- [2] K. Jain, P. Walker, N. Rowley, *Phys. Lett. B* 322 (1994) 27.
- [3] F. Kondev, G. Dracoulis, T. Kibédi, *At. Data Nucl. Data Tables* 103 (2015) 50.
- [4] E.H. Wang, J.H. Hamilton, A.V. Ramayya, et al., *Phys. Rev. C* 90 (2014) 067306.
- [5] S.J. Zhu, J.H. Hamilton, A.V. Ramayya, et al., *J. Phys. G, Nucl. Part. Phys.* 21 (1995) L57.
- [6] G.S. Simpson, W. Urban, J. Genevey, et al., *Phys. Rev. C* 80 (2009) 024304.
- [7] Z. Patel, P.-A. Söderström, Z. Podolyák, et al., *Phys. Rev. Lett.* 113 (2014) 262502.
- [8] M. Hellström, B. Fogelberg, H. Mach, et al., *Phys. Rev. C* 46 (1992) 860.
- [9] M. Hellström, H. Mach, B. Fogelberg, et al., *Phys. Rev. C* 47 (1993) 545.
- [10] X.Q. Zhang, J.H. Hamilton, A.V. Ramayya, et al., *Phys. Rev. C* 57 (1998) 2040.
- [11] C. Gautherin, M. Houry, W. Korten, et al., *Eur. Phys. J. A* 1 (1998) 391.
- [12] T. Kubo, D. Kameda, H. Suzuki, et al., *Prog. Theor. Exp. Phys.* (2012) 03C003.
- [13] Y. Yano, *Nucl. Instrum. Methods Phys. Res., Sect. B, Beam Interact. Mater. Atoms* 261 (2007) 1009.
- [14] S. Nishimura, *Prog. Theor. Exp. Phys.* 2012 (2012) 03C006.
- [15] S. Nishimura, *Nucl. Phys. News Int.* 22 (2012) 38.
- [16] P.-A. Söderström, S. Nishimura, P. Doornenbal, et al., *Nucl. Instrum. Methods Phys. Res., B* 317 (2013) 649.
- [17] K. Jain, O. Burglin, G. Dracoulis, et al., *Nucl. Phys. A* 591 (1995) 61.
- [18] P. Möller, J. Nix, W. Myers, W. Swiatecki, *At. Data Nucl. Data Tables* 59 (1995) 185.
- [19] P. Walker, G. Dracoulis, A. Byrne, et al., *Nucl. Phys. A* 568 (1994) 397.
- [20] F. Xu, P. Walker, J. Sheikh, R. Wyss, *Phys. Lett. B* 435 (1998) 257.
- [21] H.L. Liu, F.R. Xu, P.M. Walker, C.A. Bertulani, *Phys. Rev. C* 83 (2011) 011303.
- [22] R. D'Alarcao, P. Chowdhury, E.H. Seabury, et al., *Phys. Rev. C* 59 (1999) R1227.
- [23] N. Gjørup, P. Walker, G. Sletten, et al., *Nucl. Phys. A* 582 (1995) 369.
- [24] T.P.D. Swan, P.M. Walker, Z. Podolyák, et al., *Phys. Rev. C* 86 (2012) 044307.
- [25] G.D. Dracoulis, G.J. Lane, F.G. Kondev, et al., *Phys. Rev. C* 71 (2005) 044326.
- [26] G.D. Dracoulis, G.J. Lane, F.G. Kondev, et al., *Phys. Rev. C* 73 (2006) 019901.
- [27] R.O. Hughes, G.J. Lane, G.D. Dracoulis, et al., *Phys. Rev. C* 86 (2012) 054314.
- [28] T. Shizuma, K. Matsuura, Y. Toh, et al., *Nucl. Phys. A* 696 (2001) 337.
- [29] P. Walker, D. Cullen, C. Purry, et al., *Phys. Lett. B* 408 (1997) 42.